32nd EPS Conference on Plasma Phys. Tarragona, 27 June - 1 July 2005 ECA Vol.**29C**, D-1.006 (2005)

Fast Electron Bremsstrahlung in Low-Density, Grassy Sawtoothing Plasmas on JET

P. Sandquist[1], P. Helander[2], V.G. Kiptily[2], M. Lisak[1], S.E. Sharapov[2], and JET-EFDA contributors*

[1]*EURATOM-VR Association, and Department of Radio and Space Science, Chalmers University of Technology, SE-412 96 Göteborg, Sweden*

[2]*EURATOM/UKAEA Fusion Association, Culham Science Centre, Abingdon, UK*

See the Appendix of J.Pamela et al., Fusion Energy 2004 (Proc. 20th Int. Conf. Vilamoura, 2004) IAEA, Vienna (2004)

1 Introduction

Sawtooth stabilisation experiments in low-density plasmas with high-power ICRH were performed on JET showing rather dramatic results as compared to earlier studies of sawtooth stabilisation [1]. In these plasmas with high fast-ion energy content and high electron temperature, a density threshold was found about $n_e(0) \approx 2 \cdot 10^{19}$ m^{-3}, below which *monster* sawtooth stabilisation was lost and short-period, sometimes chaotic sawtooth oscillations, so-called *grassy sawteeth*, appeared instead.

In these discharges, the electric field at the magnetic axis, $E(0)$, is close to the critical electric field E_{crit} for runaway electron generation. This suggests that the transition to grassy sawteeth may be affected by a population of supra-thermal electrons enhanced by an electric field caused by sawtooth reconnection, $E_{\text{saw}} \sim |E(0) - E_{\text{crit}}|$ at $q = 1$, and sensitive to the plasma density [2,3]. Experimental evidence for supra-thermal electron generation is supported by the observation of 1) bursts of supra-thermal Electron Cyclotron Emission (ECE) at approximately each sawtooth crash, and 2) Fast Electron Bremsstrahlung (FEB) emission measured by the 19–channel FEB camera and the FEB spectrometer. The focus of this paper is to analyse the increase in average FEB intensity in the energy range 150–300 keV up to a factor of eight during the transition from ohmic to grassy sawteeth and to estimate the energy of supra-thermal electrons causing such intensity of FEB.

2 Experimental Data

The transition from grassy sawteeth to Ohmic/monster sawteeth is observed in many discharges and is controlled by a density increase from NBI or a gas puff. However, the use of NBI pollutes the FEB detectors by neutrons. Here, we analyse the transition from ohmic sawteeth to grassy sawteeth in JET shot no. 62463 with ICRH only heating (no NBI), where no pollution by neutrons entering the collimators of the FEB camera was present. Data for JET shot no. 62463 is presented in Figure 1, which shows that a transition from Ohmic sawteeth during the heating ramp-up phase to grassy sawteeth occurs at around $t = 7.5$ s. This JET shot had a magnetic field on axis $B = 2.7$ T, a plasma current $I_p = 2.5$ MA and on-axis ICRH hydrogen minority heating at a frequency $f_{\text{ICRH}} = 42$ MHz. The diagnostic tool used for measuring changes in supra-thermal electron bremsstrahlung is the FEB camera shown in Figure 2. The FEB camera gives 2D profiles of fast electron bremsstrahlung and gamma rays by using 10 horizontal and 9 vertical channels in a poloidal cross section of the JET plasma. The spatial separation between horizontal or vertical channels is ~20 cm in the centre of the plasma, whereas the temporal resolution is 10 ms. The FEB camera had three different energy windows allowing measurements over three different ranges of energy. In the sawtooth stabilisation experiments analysed here, the energy windows were defined as: FEB1 $\in [150, 300]$ keV, FEB2 $\in [300, 450]$ keV,

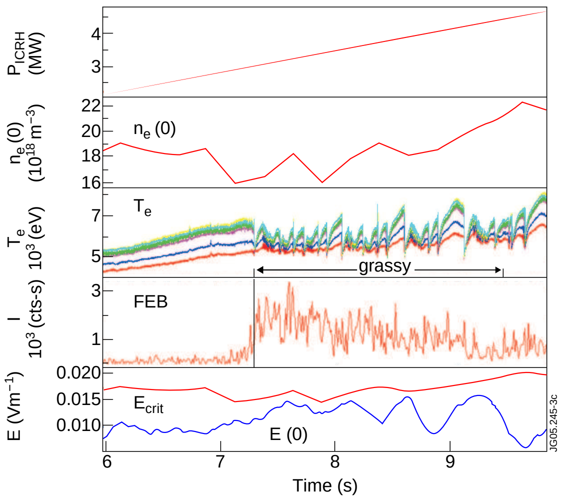

Figure 1: Top to bottom: Temporal evolutions of ICRH power, central thermal electron density measured by LIDAR, thermal electron temperature measured by ECE, fast electron bremsstrahlung for energies $[150, 300]$ keV from the FEB camera, and estimated elecric field on axis $E(0)$ and calculated critical electric field $E_{\rm crit}$. A sharp increase in fast electron bremsstrahlung emission is seen at the transition from ohmic to grassy sawteeth, when $E(0)$ approaches $E_{\rm crit}$. JET shot no. 62463.

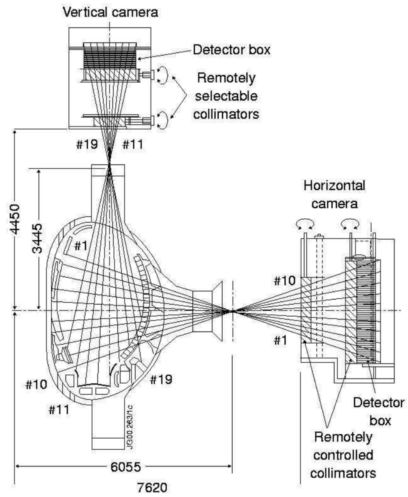

Figure 2: The Fast Electron Bremsstrahlung camera — the diagnostic tool measuring the supra-thermal electron bremsstrahlung. The 10 horizontal and 9 vertical channels have their line–of–sight through a poloidal cross section of the JET plasma.

and FEB4 > 4 MeV. For our analysis of fast electron bremsstrahlung from supra-thermal electrons the FEB1 energy window is of interest as electrons with $E \gtrsim 500$ keV emit in a narrow cone along their trajectory not detectable with the FEB camera with lines-of-sight perpendicular to the magnetic axis.

When using the FEB camera as the diagnostic tool for analysing supra-thermal electrons in the central part of the plasma, hot spots and other edge phenomena giving large emission bursts detected by the FEB camera must be filtered out. This filtering was performed by using a correlation function between central vertical and central horizontal channels. 2D profiles of bremsstrahlung radiation and gamma rays are reconstructed with tomography, filtering out the hot spots. The reconstructed profiles use one second averaging time and they are found to be non-monotonic during the grassy sawtooth phase as Figure 3 shows. From the tomographic reconstructions in the low energy window, $[150, 300]$ keV, one can observe a time-averaged population of fast electrons around $r/a \approx 0.2 \div 0.3$ close to $q = 1$. The two higher energy windows, showing gamma-ray emission from trapped fast ions, show emission of a different geometry and are unlikely to pollute the lower-energy FEB profile.

The existence of suprathermal generation is also observed in the ECE data shown in Figure 4. Clear bursts of supra-thermal ECE are observed in the outer ECE channels (corresponding to $2^{\rm nd}$ harmonic X-mode emission with resonant magnetic fields located outside the plasma). This figure clearly demonstrates the generation of runaways at the sawtooth crashes, from which an enhanced supra-thermal electron tail of the distribution function is deduced. We note, however, that the essentially different temporal evolutions of the FEB and ECE signals is a consequence of the different sensitivity of the two diagnostics to the supra-thermal electrons. While the FEB diagnostic is sensitive to both parallel and perpendicular energy distributions of the supra-thermal electrons, 2^{nd} harmonic X-mode supra-thermal ECE gives information about the fast perpendicular energy component.

Finally, the single line-of-sight FEB spectrometer measuring $I_\gamma(E_\gamma)$ showed an exponential decrease in E_γ, from which an electron temperature of approximately 80 keV can be obtained. The existence of supra-thermal electrons is thus experimentally deduced in several ways.

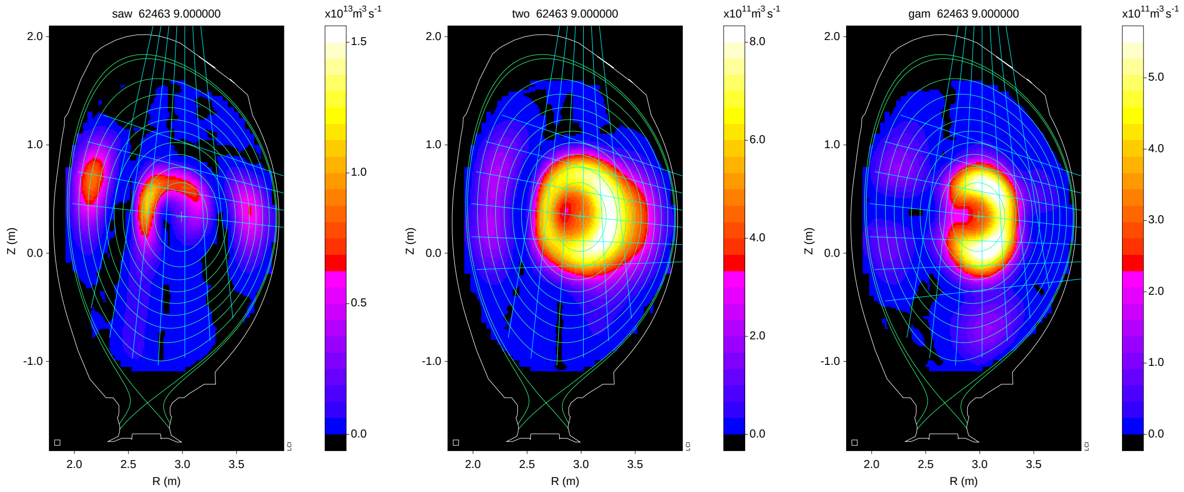

(a) (b) (c)

Figure 3: Left to right: Tomographic reconstructions of FEB camera data in the energy intervals $[150, 300]$ keV, $[300, 450]$ keV and > 4 MeV, respectively. The low energy data in (a) shows a hollow fast electron bremsstrahlung profile with a time-averaged population of fast electrons around $r/a \approx 0.2 \div 0.3$ close to $q = 1$. The data in (b) has a large part caused by Thomson scattering of higher-energy gamma rays, but also a part in the inner side of the torus, which cannot be interpreted as the result of Thomson scattering. Finally, the highest energy data in (c) shows the characteristic banana orbits of the ICRH-accelerated ions, in full agreement with the topology of trapped fast ions. JET shot no. 62463.

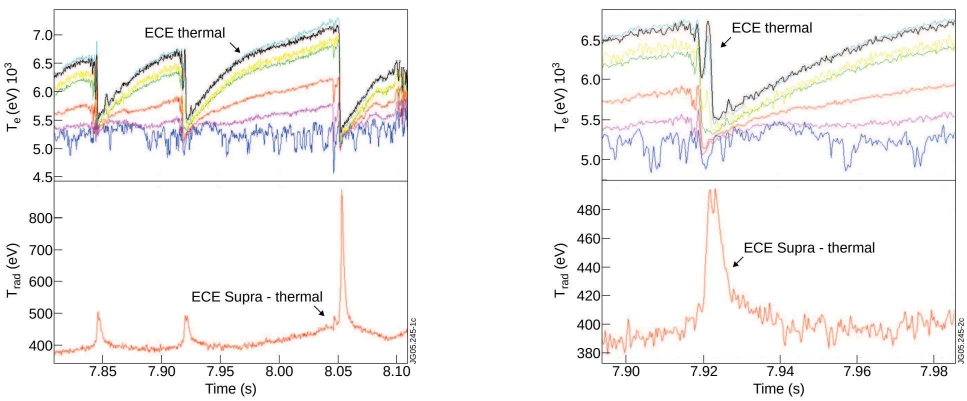

(a) (b)

Figure 4: Bursts of supra-thermal Electron Cyclotron Emission are observed at each grassy sawtooth crash, indicating the generation of fast electrons upon reconnection. The top figures of (a) and (b) show the temporal evolution of the central ECE channels (thermal emission), whereas the bottom figures of (a) and (b) show an ECE channel located outside the plasma (non-thermal emission). JET shot no. 62463.

3 Bremsstrahlung of Supra-Thermal Tail

In this analysis, possible effects of secondary fast electrons (avalanches) are neglected. In order to calculate the emission of fast electron bremsstrahlung numerically, we need to know the relativistic electron distribution function, since $E_\gamma \lesssim m_0c^2$. We perform a similar analysis as in [2] and extend the analysis in region III to our case $\alpha = E(0)/E_{\rm crit} \lesssim 1$ — see Figure 1. We calculate the tail of the electron distribution function, $\delta f_{\rm e}(q)$, with $q = p/m_{\rm e}c$, where p is the parallel to $E(0)$ component of the momentum [2], and use this expression for the tail in the bremsstrahlung calculations.

The fast electron bremsstrahlung emission, N, is calculated from

$$N = \int_{l_{\min}}^{l_{\max}} {\rm G}(l){\rm d}l \int_{Q_{\min}}^{Q_{\max}} {\rm d}Q \int_0^{d_{S_1}^2/16l^2} {\rm d}\Omega \int_{E_{\gamma,\min}}^{E_{\gamma,\max}} {\rm d}E_\gamma \int_{q_{{\rm e},\min}(E_\gamma)}^{\sqrt{3}} {\rm d}q \frac{{\rm d}^3N}{{\rm d}E_\gamma {\rm d}\Omega {\rm d}Q} n_{\rm i} v_{\rm e} \delta f_{\rm e}(q) \ , \qquad (1)$$

where the differential radiation cross section [4]

$$\frac{{\rm d}^3N}{{\rm d}E_\gamma {\rm d}\Omega {\rm d}Q} = \{z=1, \theta = \frac{\pi}{2}\} = \frac{1}{\pi}\frac{Z_{\rm eff}^2 e^6}{m_{\rm e}^2 c^5 \beta^2 \hbar E_\gamma Q}(1+\beta^2)\gamma^{-2} \qquad (2)$$

and the geometry factor ${\rm G}(l)$ [5] have been introduced. Normalised momentum is introduced according to $\beta = |\mathbf{p}|/\gamma m_{\rm e}c$.

Substituting the characteristic (mean) values of critical field parameter α and expansion parameter $\epsilon = T_{\rm e}/m_{\rm e}c^2$, in both ohmic and grassy sawteeth regimes, and using a thermal temperature of 6 keV in the ohmic regime and the spectrometer-deduced temperature of 80 keV in the grassy regime, respectively, to estimate the electron velocity $v_{\rm e}$, into Equation 1 we numerically obtain for average distribution functions $N_{\rm grassy}/N_{\rm ohmic} \cong 5.5$, while the experimental increase of FEB emission is up to a factor of eight.

4 Conclusions

The existence of supra-thermal electrons during the grassy sawteeth regime is experimentally verified through increased Fast Electron Bremsstrahlung emission. The increase in FEB emission in the transition from Ohmic to grassy sawteeth is qualitatively reproduced by an averaged numerical bremsstrahlung calculation for the two sawteeth regimes. The supra-thermal Electron Cyclotron Emission bursts at each grassy sawtooth, the geometry of the emission in the tomographic reconstructions of the three FEB energy windows and the electron temperature deduced from the single line-of-sight FEB spectrometer further support the existence of supra-thermal electrons. Future work aims to include the correct time-dependencies of the variables α and ϵ supported by better time-resolved FEB measurements, and to study effects of supra-thermal electrons on sawtooth stability.

Acknowledgements

This work has been conducted under the European Fusion Development Agreement and has been funded by EURATOM, Vetenskapsrådet and EPSRC.

References

[1] M.J. Mantsinen et al., Plasma Phys. Control. Fusion **42**, 1291 (2000).
[2] J.W. Connor and R.J. Hastie, Nucl. Fusion **15**, 415 (1975).
[3] P.V. Savrukhin et al., Proceed. $28^{\rm th}$ EPS Conf. on Contr. Fus. and Plasma Phys. Funchal, 18-22 June 2001, ECA Vol. **25A**, 1421 (2001).
[4] J.D. Jackson, *Classical Electrodynamics*, Wiley New York (1975).
[5] P. Froissard, *Ph D Thesis*, Université de Provence Aix-Marseille I (1992).